

Scalable Knowledge Editing for Mixture-of-Experts LLMs via Tensor-Structured Updates

Roman Maksimov^{1,2}, Vladimir Aletov^{1,2}, Dmitry Bylinkin^{1,2}, Daniil Medyakov^{1,2}, Vladimir Solodkin^{1,2}, Aleksandr Beznosikov^{1,2,3}

¹Moscow Independent Research Institute of Artificial Intelligence

²Basic Research of Artificial Intelligence Laboratory

³Innopolis University

Knowledge editing (KE) provides a lightweight alternative to repeated fine-tuning of LLMs. However, most existing KE methods target dense feed-forward layers, while modern LLMs increasingly adopt Mixture-of-Experts (MoE) architectures for their superior memory footprint and inference efficiency. This mismatch leaves a growing class of production models without principled editing tools. We propose a MEMIT-like framework for knowledge editing in MoE-based LLMs. Our method exploits the tensor structure of MoE layers to formulate the editing objective faithfully at the per-expert level, and applies the Woodbury matrix identity to avoid materializing or inverting the full stacked matrix of expert weights. The resulting update reduces to inversions of fixed low-rank matrices and requires no additional backward passes. Empirically, our approach matches the editing quality of strong baselines on the main KE metrics while accelerating the editing procedure by up to 6x, owing to the batched MEMIT-style formulation and the low-dimensional inversions enabled by the Woodbury identity. These results show that closed-form, parameter-modifying KE can be extended efficiently beyond dense layers, opening a path toward scalable knowledge editing in modern sparse LLM architectures.

1 Introduction

Large language models (LLMs) have become foundational tools in a wide range of natural language processing applications. However, the factual knowledge encoded in their parameters is inherently static once training concludes, while the world in which they are deployed is not. Maintaining factual accuracy through repeated fine-tuning is prohibitively expensive at the scale of modern LLMs. This holds even for parameter-efficient methods, which still require substantial compute and curated training data [Mitchell et al., 2021] and which risk catastrophic forgetting of previously acquired knowledge when applied repeatedly [Luo et al., 2025].

Knowledge editing (KE) [Wang et al., 2024b] has emerged as a principled response to this challenge. Rather than retraining the model, KE methods aim to inject or overwrite individual factual associations through targeted modifications of model parameters or auxiliary modules. A particularly successful line of work, represented by ROME [Meng et al., 2022a] and its batched extension MEMIT [Meng et al., 2022b], formulates editing as a closed-form least-squares update on the down-projection matrix of a feed-forward (FFN) layer, treated as a linear associative memory [Anderson, 1972; Geva et al., 2021; Sun et al., 2024]. These methods are attractive because they are fast, they do not require gradient-based optimization of the edited weights, and admit a clean theoretical interpretation.

Following MEMIT [Meng et al., 2022b], the field of knowledge editing has developed along several complementary directions. The most relevant to our work is the line that refines the closed-form *locate-and-edit* paradigm:

PMET [Li et al., 2024] jointly optimizes the hidden states of both MHSA and FFN sublayers but uses only the FFN component for the weight update, yielding more precise edits, while EMMET [Gupta et al., 2024] unifies ROME and MEMIT under a common preservation–memorization objective and proposes a batched equality-constrained variant. Within the same line, AlphaEdit [Fang et al., 2024] addresses the degradation of locate-and-edit methods under long sequences of edits by projecting each parameter perturbation onto the null-space of the preserved knowledge, thereby preventing interference between successive updates and substantially improving stability in the sequential-editing regime. Beyond this paradigm, complementary directions include tackling the reversal curse via bidirectional editing objectives [Ma et al., 2023], memory-based approaches that keep the base weights untouched and attach an external codebook or side memory [Hartvigsen et al., 2023; Wang et al., 2024a], and regularization-based methods that preserve the model’s general abilities under many edits [Gu et al., 2024].

A critical limitation is that essentially all closed-form parameter-editing methods have been developed and evaluated on *dense* transformer architectures. Modern leading LLMs increasingly depart from this regime: state-of-the-art systems such as GPT-OSS [OpenAI, 2025], DeepSeek-v4 [DeepSeek-AI, 2026], and Qwen3.6 [Qwen Team, 2026] adopt **Mixture-of-Experts** (MoE) designs [Shazeer et al., 2017; Molodtsov et al., 2026], in which the dense FFN is replaced by a router and a pool of experts, only a small subset of which is activated per token. MoE architectures dominate the current frontier for a clear reason: they decouple parameter count from per-token compute. This enables dramatically larger capacity at fixed inference cost. As a result, in modern MoE-based LLMs, the parameters that previously stored factual associations in dense FFNs are now distributed across a pool of experts gated by a router [Zhao et al., 2024]. This mismatch raises a concrete and underexplored question:

How can closed-form, parameter-modifying knowledge editing be performed faithfully and efficiently in MoE-based LLMs?

To the best of our knowledge, the only method developed specifically for this setting is MoE-Edit [Gu et al., 2026]. It reformulates the KE objective in a way that faithfully accounts for the MoE structure, and solves the resulting problem by applying MEMIT-like updates. Within each layer, an approximate block coordinate descent (BCD) procedure iterates over experts one at a time, computing per-expert updates that are subsequently projected onto the null-space of the preserved knowledge, following the AlphaEdit [Fang et al., 2024] formulation. However, this design imposes a twofold sequential bottleneck: *(i)* activation collection must be repeated layer by layer for every batch of edits, while within each layer *(ii)* the BCD solver iterates sequentially over experts. As the number of edits and the number of experts grow, both factors compound and make the procedure increasingly expensive, motivating a closed-form alternative.

Contributions. In this work, we propose a novel framework tailored to MoE architectures. Our contributions are as follows:

- We formulate the knowledge editing objective for MoE layers in a way that respects the tensor structure of stacked expert weights, avoiding both single-expert and naively concatenated dense surrogates. Exploiting this structure, we recast the problem into a form where the Woodbury identity applies efficiently, yielding a closed-form update that never materializes or inverts the full stacked expert matrix and requires only inversions of size fixed by the number of edits.
- The resulting update rule of **MoE Tucker Editor** (MoTE) is fully closed-form and **backward-pass-free**: like MEMIT in the dense case, it requires no gradient computation through the edited layer and inherits the batched-edit property that makes MEMIT practical at scale.
- Empirically, MoTE achieves editing quality comparable to strong baselines on efficacy, generalization, and specificity, while accelerating the editing procedure by **up to 6×**. This speedup is achieved by collecting activations only once at the last layer and finding closed form solution only once for that last layer.

The remainder of the paper is organized as follows. Section 2 introduces background on MEMIT and the structure of MoE FFN layers. Section 3 presents our method. Section 4 reports experimental results on standard KE benchmarks, and Section 6 concludes with a discussion of limitations and future directions.

2 Preliminaries

2.1 Algebraic prerequisites

The Woodbury identity. Let $A \in \mathbb{R}^{n \times n}$ be invertible, $U \in \mathbb{R}^{n \times T}$, $V \in \mathbb{R}^{T \times n}$, and $C \in \mathbb{R}^{T \times T}$ invertible. The Woodbury identity [Hager, 1989; Duncan, 1944] states

$$(A + UCV)^{-1} = A^{-1} - A^{-1}U(C^{-1} + VA^{-1}U)^{-1}VA^{-1}.$$

Specializing $A = \lambda I_n$, $C = I_T$, $U = \Psi$, and $V = \Psi^\top$ yields the *push-through corollary*:

$$\Psi^\top(\Psi\Psi^\top + \lambda I_n)^{-1} = (\Psi^\top\Psi + \lambda I_T)^{-1}\Psi^\top, \quad \forall \lambda > 0, \Psi \in \mathbb{R}^{n \times T}, \quad (1)$$

which trades an $n \times n$ inversion for a $T \times T$ inversion at the cost of two matrix multiplications.

Tucker Decomposition. Let $\mathcal{X} \in \mathbb{R}^{I_1 \times I_2 \times \dots \times I_N}$ be an N -th order tensor. A *Tucker decomposition* [Tucker, 1963] factors \mathcal{X} into a smaller *core tensor* $\mathcal{G} \in \mathbb{R}^{R_1 \times R_2 \times \dots \times R_N}$ multiplied along each mode by a *factor matrix* $U^{(n)} \in \mathbb{R}^{I_n \times R_n}$:

$$\mathcal{X} \approx \mathcal{G} \times_1 U^{(1)} \times_2 U^{(2)} \times_3 \dots \times_N U^{(N)}, \quad (2)$$

where \times_n denotes the mode- n product. The tuple (R_1, \dots, R_N) is the *multilinear rank* of the decomposition. Choosing $R_n < I_n$ enforces a low-rank structure along mode n . The factors $U^{(n)}$ are typically required to have orthonormal columns, in which case (2) is known as the *higher-order SVD* (HOSVD) [De Lathauwer et al., 2000], computed by truncating the SVD of each unfolding $X_{(n)}$.

Tucker decompositions in deep learning. Tucker decomposition has long served as a structural prior on neural-network parameters. The natural modes of trained neural-network weight tensors – channels, layers, heads, or experts – exhibit a multilinear rank far below their nominal dimension [Gu et al., 2025; Peshekhonov et al., 2024; Li et al., 2026; Yuebin et al.].

2.2 Dense FFN as a Linear Associative Memory

A standard Transformer block alternates a multi-head self-attention (MHSA) sublayer with a position-wise feed-forward network (FFN). In modern gated variants, the FFN consists of three linear maps: an *up-projection* $W_{\text{up}} \in \mathbb{R}^{d_{\text{hidden}} \times d_{\text{model}}}$, a *gate projection* $W_{\text{gate}} \in \mathbb{R}^{d_{\text{hidden}} \times d_{\text{model}}}$, and a *down-projection* $W_{\text{down}} \in \mathbb{R}^{d_{\text{model}} \times d_{\text{hidden}}}$.

Following [Geva et al., 2021; Meng et al., 2022a], the down-projection admits a natural interpretation as a *linear associative memory*: each of its d_{hidden} columns acts as a value vector associated with a learned key direction in the gated activation space. Concretely, given a hidden state $u \in \mathbb{R}^{d_{\text{model}}}$, the FFN first builds a key

$$k = \sigma(W_{\text{gate}} u) \odot (W_{\text{up}} u) \in \mathbb{R}^{d_{\text{hidden}}},$$

where $\sigma(\cdot)$ is a non-linearity and \odot denotes the Hadamard product. The FFN output is then a linear combination of the columns of W_{down} weighted by k :

$$v = W_{\text{down}} k \in \mathbb{R}^{d_{\text{model}}}.$$

Knowledge editing as a regularized least-squares problem. Knowledge editing seeks to install a new association into this memory. For a target fact (s, r, o_{new}) – a subject s , a relation r , and a desired new object o_{new} – the goal is to modify the model so that the key $k_{(s,r)}$ corresponding to the prompt encoding (s, r) is mapped to a new target vector $z \in \mathbb{R}^{d_{\text{model}}}$ that steers downstream computation toward o_{new} . Two competing requirements must be balanced. The update should be *effective* on the edited fact and its paraphrases (efficacy and generalization), and *local*, i.e. leave the model’s predictions on unrelated inputs essentially unchanged (specificity).

In the dense case, this trade-off is naturally expressed as a regularized least-squares problem over an additive perturbation $\Delta \in \mathbb{R}^{d_{\text{model}} \times d_{\text{hidden}}}$:

$$\Delta^* = \arg \min_{\Delta} \underbrace{\|(W_{\text{down}} + \Delta) K_1 - V_1\|_F^2}_{\text{memorization}} + \underbrace{\|\Delta K_0\|_F^2}_{\text{preservation}} + \lambda \|\Delta\|_F^2, \quad (3)$$

where $K_1 \in \mathbb{R}^{d_{\text{hidden}} \times T}$ stacks the keys of the T edited facts column-wise, $V_1 \in \mathbb{R}^{d_{\text{model}} \times T}$ contains the corresponding target values, and $K_0 \in \mathbb{R}^{d_{\text{hidden}} \times M}$ is a preservation key set sampled from the model’s empirical activation distribution on a large generic corpus. The Frobenius regularizer $\lambda > 0$ controls the magnitude of the update. Problem (3) admits a closed-form solution involving only a single $d_{\text{hidden}} \times d_{\text{hidden}}$ inversion, which underlies the ROME [Meng et al., 2022a] and MEMIT [Meng et al., 2022b] families of methods.

2.3 MoE Layer as a Mixture of Expert Associative Memories

Modern frontier LLMs replace the dense FFN with a *Mixture-of-Experts* (MoE) sublayer [Shazeer et al., 2017; Lepikhin et al., 2020; Du et al., 2022]. The motivation is well known: MoE decouples a model’s parameter count from its per-token compute. A pool of E specialized FFN-shaped experts collectively stores far more parameters than a dense FFN of the same compute budget, while only $K \ll E$ of them are activated per token via a sparse routing mechanism.

Router. At the core of the layer is a *router*, a lightweight learned function that determines which experts process each token. Given an input hidden state $x \in \mathbb{R}^{d_{\text{model}}}$, the router produces affinity logits with respect to E learned expert embeddings $e_1, \dots, e_E \in \mathbb{R}^{d_{\text{model}}}$:

$$s_j = x^\top e_j, \quad j = 1, \dots, E.$$

A top- K operator selects the indices of the K largest logits,

$$S = \text{TopK}(\{s_1, \dots, s_E\}) \subset \{1, \dots, E\}, \quad |S| = K,$$

and the corresponding logits are renormalized into a sparse gating distribution over the selected experts:

$$g_j = \begin{cases} \frac{\exp(s_j)}{\sum_{\ell \in S} \exp(s_\ell)}, & j \in S, \\ 0, & j \notin S. \end{cases} \quad (4)$$

By construction, $\sum_j g_j = 1$ and the gating vector $\mathbf{g} = (g_1, \dots, g_E)$ is K -sparse.

Experts. Each expert $j \in \{1, \dots, E\}$ implements a self-contained gated FFN with its own parameters $(W_{\text{gate}}^{(j)}, W_{\text{up}}^{(j)}, W_{\text{down}}^{(j)})$. By analogy with the dense case, expert j first computes its own key

$$k_j = \sigma(W_{\text{gate}}^{(j)} x) \odot (W_{\text{up}}^{(j)} x) \in \mathbb{R}^{d_{\text{hidden}}},$$

and then produces its contribution by reading out from its own associative memory:

$$v_j(x) = W_j k_j, \quad W_j := W_{\text{down}}^{(j)} \in \mathbb{R}^{d_{\text{model}} \times d_{\text{hidden}}}.$$

Crucially, both the keys k_j and the values v_j are expert-specific: different experts construct different gated activations from the same input u and project them through different down-projections.

Mixture output. The output of the MoE layer is the router-weighted sum of the contributions of the active experts

$$v = \sum_{j=1}^E g_j v_j = \sum_{j \in S} g_j W_j k_j, \quad (5)$$

where the second equality follows from the sparsity of \mathbf{g} in (4). Equation (5) makes explicit the structural property that distinguishes MoE editing from the dense case: a single MoE layer is no longer one associative memory W_{down} , but a *mixture of E associative memories* $\{W_j\}_{j=1}^E$, dynamically combined per token by the router.

Closed-form MoE editing objective. [Gu et al., 2026] recently extended the dense formulation (3) to MoE layers. Treating the per-expert down-projections $\{W_j\}_{j=1}^E$ jointly as the optimization variable, they cast knowledge editing as the following block-structured regularized problem:

$$\{\Delta_j^*\}_{j=1}^E = \arg \min_{\{\Delta_j\}} \sum_{f \in \mathcal{F}} \left\| \sum_{j=1}^E g_{f,j} (W_j + \Delta_j) k_{f,j} - v_f \right\|^2 + \sum_{f \in \mathcal{P}} \left\| \sum_{j=1}^E g_{f,j} \Delta_j k_{f,j} \right\|^2 + \lambda \sum_{j=1}^E \|\Delta_j\|^2, \quad (6)$$

where \mathcal{F} is the set of facts to edit, \mathcal{P} the preservation set, and $g_{f,j}$, $k_{f,j}$ the router weight and expert-specific key induced by prompt f on expert j . Stacking the per-expert updates into the vector $\theta = \text{vec}([\Delta_1 \cdots \Delta_E])$ and defining the per-fact design vector

$$\psi_f = [g_{f,1} k_{f,1}^\top \cdots g_{f,E} k_{f,E}^\top]^\top \in \mathbb{R}^{E d_{\text{hidden}}}, \quad r_f = v_f - \sum_{j=1}^E g_{f,j} W_j k_{f,j},$$

problem (6) admits the closed-form solution

$$\theta^* = \left(\sum_{f \in \mathcal{F}} (\psi_f \psi_f^\top) \otimes I_{d_{\text{model}}} + \lambda I \right)^{-1} \sum_{f \in \mathcal{F}} (\psi_f \otimes I_{d_{\text{model}}}) r_f, \quad (7)$$

$$\Delta^* = \text{unvec}(\theta^*), \quad (8)$$

where \otimes denotes the Kronecker product. Although elegant, this global solution requires inverting a system of size $(E d_{\text{hidden}}) \times (E d_{\text{hidden}})$, which is computationally prohibitive at realistic scales. This limitation motivates the block-coordinate treatment developed in the MoE-Edit work.

3 Method

Section 2 ended with the closed-form MoE editing objective (6), whose unique global minimizer requires solving a linear system of size $(E d_{\text{hidden}}) \times (E d_{\text{hidden}})$ – intractable at modern MoE scales. We construct MoTE by composing three ingredients. (i) A *Woodbury reduction* that shrinks the per-layer inversion to size $T \times T$, where T is the number of edits in a batch, independent of E and d_{hidden} . (ii) A *MEMIT-style updates schedule* that replaces the per-layer solve with spreading deltas across layers. (iii) A *Tucker reparameterization* of the update tensor $\Delta W \in \mathbb{R}^{E \times d_{\text{model}} \times d_{\text{hidden}}}$ that respects the underlying geometric structure of the MoE down-projection. As we show in Section 3.1, the first ingredient in cope with MEMIT residual schedule can yield a direct MoE adaptation that is computationally tractable but empirically uncompetitive; ingredients (ii) and (iii), developed in Section 3.3, supply the missing structural prior and provide significant speed-up.

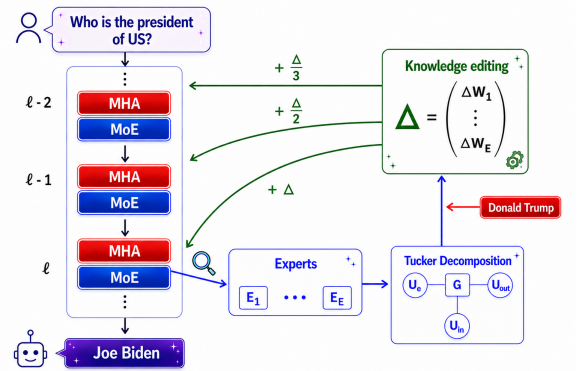


Figure 1: MoTE editing pipeline

3.1 Woodbury Reduction and Multi-layer Spread

The closed-form solution of (6) requires inverting a system of size $(E d_{\text{hidden}}) \times (E d_{\text{hidden}})$, with time and memory costs of $\mathcal{O}((E d_{\text{hidden}})^3)$ and $\mathcal{O}((E d_{\text{hidden}})^2)$ respectively. However, the Gram matrix driving the inversion is structurally low-rank: it is a sum of $T = |\mathcal{F}|$ rank-one terms $\psi_f \psi_f^\top$, where T – the number of edits processed in a batch – is several orders of magnitude smaller than $E d_{\text{hidden}}$. This is precisely the regime in which the Woodbury identity (1) converts the inversion into a much smaller one.

Stacking the per-fact design vectors and target residuals as

$$\Psi = [\psi_1 \cdots \psi_T] \in \mathbb{R}^{E d_{\text{hidden}} \times T}, \quad R = [r_1 \cdots r_T] \in \mathbb{R}^{d_{\text{model}} \times T},$$

and unvectorizing θ^* into the matrix $\hat{\Delta}^* = [\Delta_1^* \cdots \Delta_E^*] \in \mathbb{R}^{d_{\text{model}} \times E d_{\text{hidden}}}$, the global minimizer of (6) reads

$$\hat{\Delta}^* = R \Psi^\top (\Psi \Psi^\top + \lambda I_{E d_{\text{hidden}}})^{-1}.$$

Substituting the push-through corollary (1) into the rightmost factor yields the equivalent but computationally far cheaper expression

$$\boxed{\hat{\Delta}^* = R (\Psi^\top \Psi + \lambda I_T)^{-1} \Psi^\top.} \quad (9)$$

The only matrix to invert is now of size $T \times T$, independent of both the number of experts E and the expert hidden dimension d_{hidden} . Concretely, (9) requires forming the kernel matrix $\Psi^\top \Psi \in \mathbb{R}^{T \times T}$ in $\mathcal{O}(T^2 E d_{\text{hidden}})$ time, factorizing a $T \times T$ system in $\mathcal{O}(T^3)$ time, and assembling $\hat{\Delta}^*$ via two dense products in $\mathcal{O}(T d_{\text{model}} E d_{\text{hidden}})$ time.

Plugging Woodbury into a MEMIT-style multi-layer editor. Equation (9) solves the editing problem at a single critical layer, but locate-then-edit methods derive most of their leverage by spreading an edit across several layers. The naive and natural approach here is to adapt the standard MEMIT [Meng et al., 2022b] schedule. Having solved (6) at the topmost critical layer L via (9), we obtain per-fact target residuals

$$r_f^L = v_f - \sum_{j=1}^E g_{f,j}^L W_j^L k_{f,j}^L,$$

each of which already aggregates the contributions of all E experts at layer L . We then propagate the edit downward by spreading these residuals across the preceding critical layers $\ell \in \{L_0, \dots, L\}$ with a coefficient that decays with the distance from L :

$$r_f^\ell = \frac{r_f^L}{L - \ell + 1}, \quad \hat{\Delta}^{\ell,*} = R^\ell (\Psi^L)^\top (\Psi^L (\Psi^L)^\top + \lambda I)^{-1}, \quad (10)$$

where $R^\ell = [r_f^\ell]_{f \in \mathcal{F}} \in \mathbb{R}^{d_{\text{model}} \times T}$ stacks the per-layer residuals. Direct adaptation of MEMIT would require substituting Ψ^L in (10) with $\Psi^\ell \in \mathbb{R}^{E d_{\text{hidden}} \times T}$ which stacks the per-fact design vectors $\psi_f^\ell = [g_{f,1}^\ell k_{f,1}^{\ell \top} \cdots g_{f,E}^\ell k_{f,E}^{\ell \top}]^\top$ – the same construction as in (6), but with the router weights $g_{f,j}^\ell$ and per-expert keys $k_{f,j}^{\ell}$ recomputed at layer ℓ , since both the routing distribution and the expert activations differ from layer to layer. Opposite to that, our approach allows to avoid additional computations by calculating the solution only once at the last layer and spreading it across previous layers with the same schedule. The denominator $L - \ell + 1$ assigns the largest share to the layer closest to L and gradually attenuates earlier layers, mirroring the original MEMIT schedule. Crucially, each per-layer solve in (10) has the form addressed by (9): applying push-through gives the equivalent $\hat{\Delta}^{\ell,*} = R^\ell ((\Psi^L)^\top \Psi^L + \lambda I_T)^{-1} (\Psi^L)^\top$, so the only matrices ever inverted across the entire multi-layer pipeline are of size $T \times T$. In this sense, the Woodbury reduction makes possible a direct MoE port of MEMIT – and, more broadly, of any locate-then-edit method that relies on an analogous closed-form ridge solve – computationally tractable out of the box.

3.2 The Tensor-Structure Diagnosis

An empirical surprise. Despite its apparent elegance, the direct combination of the Woodbury reduction (9) with the MEMIT-style multi-layer spread (10) fails to deliver competitive editing quality on MoE backbones. As we report in Section 4, this naive adaptation lags substantially behind dense-model expectations on the evaluation. This raises a natural question:

What aspect of the MoE architecture is this otherwise principled recipe failing to account for?

We argue that the diagnosis is structural rather than algorithmic. By stacking the per-expert updates $\{\Delta_j\}_{j=1}^E$ into a flat matrix $\hat{\Delta} \in \mathbb{R}^{d_{\text{model}} \times E d_{\text{hidden}}}$, problem (6) implicitly treats the E experts as independent blocks of an otherwise unstructured linear map. The natural object underlying an MoE layer, however, is not a matrix but a third-order tensor: the per-expert down-projections $\{W_j\}_{j=1}^E$ assemble into

$$\mathcal{W} \in \mathbb{R}^{E \times d_{\text{model}} \times d_{\text{hidden}}},$$

and the corresponding updates are naturally represented as tensors $\Delta\mathcal{W}$. Experts within the same layer are far from arbitrary: they share substantial structure inherited from joint pretraining. The flat block-diagonal solve of (10) discards this structure entirely, spending its regularization budget on update directions that lie *outside* the low-multilinear-rank manifold along which experts actually vary; symmetrically, perturbations along that manifold are damped by the Frobenius regularizer at the same rate as genuinely unstructured noise. This observation motivates a tensor-aware reformulation, in which the unknown $\Delta\mathcal{W}$ is sought directly in factored form. A Tucker decomposition [Tucker, 1963] is the canonical choice: it disentangles the three modes – expert, model, and hidden – through a small core tensor \mathcal{G} and three mode-specific factor matrices, aligning the optimization variable with the multilinear geometry of the MoE layer.

3.3 Tucker-Structured MoE Editor

We now combine the two ingredients on the table. The Woodbury reduction of Section 3.1 makes a per-layer MEMIT solve cheap in the unstructured case, while the diagnosis of Section 3.2 indicates that the unstructured solve is the wrong object: experts co-vary along a low-multilinear-rank manifold of \mathcal{W} . We constrain the editing update $\Delta\mathcal{W}$ to live on the Tucker manifold of \mathcal{W} itself, and solve the resulting MEMIT objective in closed form via the Woodbury push-through.

Stack the per-expert updates into a tensor $\Delta\mathcal{W} \in \mathbb{R}^{E \times d_{\text{model}} \times d_{\text{hidden}}}$ with $\Delta\mathcal{W}[j, :, :] = \widehat{\Delta W}_j$, and constrain it to Tucker form

$$\Delta\mathcal{W} = \mathcal{G} \times_1 U_e \times_2 U_{\text{out}} \times_3 U_{\text{in}},$$

with factors $U_e \in \mathbb{R}^{E \times r_e}$, $U_{\text{out}} \in \mathbb{R}^{d_{\text{model}} \times r_{\text{out}}}$, $U_{\text{in}} \in \mathbb{R}^{d_{\text{hidden}} \times r_{\text{in}}}$ and core $\mathcal{G} \in \mathbb{R}^{r_e \times r_{\text{out}} \times r_{\text{in}}}$, where $(r_e, r_{\text{out}}, r_{\text{in}}) \ll (E, d_{\text{model}}, d_{\text{hidden}})$. The per-expert update reads

$$\widehat{\Delta W}_j = U_{\text{out}} \left(\sum_{a=1}^{r_e} U_e[j, a] G_a \right) U_{\text{in}}^\top, \quad G_a := \mathcal{G}[a, :, :]. \quad (11)$$

The factors $U_e, U_{\text{out}}, U_{\text{in}}$ are fixed, whereas the core \mathcal{G} with $r_e r_{\text{out}} r_{\text{in}}$ free entries is optimized.

Factor extraction. We obtain $U_e, U_{\text{out}}, U_{\text{in}}$ once at initialization by HOSVD [De Lathauwer et al., 2000] on \mathcal{W} itself, computed via the Gram trick: $U_n = \text{TopEig}_{r_n}(\mathcal{W}_{(n)}\mathcal{W}_{(n)}^\top)$ for $n \in \{e, \text{out}, \text{in}\}$, optionally refined by a few HOOI [Kolda and Bader, 2009] sweeps. Following TD-MoE [Yuebin et al.], we additionally support multilinear whitening of \mathcal{W} before HOSVD using mode-wise activation covariances $\Sigma_{\text{out}}, \Sigma_{\text{in}}$, so that the factors are aligned with the data geometry rather than with the raw weight geometry; the recovered factors are subsequently recoloured to the original space. We refer to the paper [Yuebin et al.] for the full whitening recipe. Ablation on whitening types in Appendix C.2 shows that *in* regime performs the best.

Compressed editing objective. Substituting (11) into the per-layer MEMIT objective (10) collapses the $E d_{\text{model}} d_{\text{hidden}}$ -dimensional optimization onto the much smaller core \mathcal{G} . With null-space-projected keys $\tilde{k}_{t,j} = P_j k_{t,j}$, define the *compressed key* and the *expert-mode aggregate*

$$c_{t,j} = U_{\text{in}}^\top \tilde{k}_{t,j} \in \mathbb{R}^{r_{\text{in}}}, \quad \phi_{t,a} = \sum_{j=1}^E g_{t,j} U_e[j, a] c_{t,j} \in \mathbb{R}^{r_{\text{in}}},$$

and stack them as $\phi_t = [\phi_{t,1}; \dots; \phi_{t,r_e}] \in \mathbb{R}^{r_e r_{\text{in}}}$. Letting $G_{\text{flat}} = [G_1 \ \dots \ G_{r_e}] \in \mathbb{R}^{r_{\text{out}} \times r_e r_{\text{in}}}$ denote the mode-1 unfolding of \mathcal{G} , a direct calculation gives

$$U_{\text{out}}^\top \sum_{j=1}^E g_{t,j} \widehat{\Delta W}_j \tilde{k}_{t,j} = G_{\text{flat}} \phi_t,$$

so that, after compressing the per-fact target residual analogously, $\tilde{r}_t = U_{\text{out}}^\top r_t \in \mathbb{R}^{r_{\text{out}}}$, the projected MEMIT objective reduces to a ridge regression in the core variable:

$$\min_{G_{\text{flat}}} \sum_{t=1}^T \|\tilde{r}_t - G_{\text{flat}} \phi_t\|_2^2 + \lambda \|G_{\text{flat}}\|_F^2. \quad (12)$$

Let $\Phi = [\phi_1, \dots, \phi_T]^\top \in \mathbb{R}^{T \times r_e r_{\text{in}}}$ and $\tilde{R} = [\tilde{r}_1, \dots, \tilde{r}_T]^\top \in \mathbb{R}^{T \times r_{\text{out}}}$. The normal equations of (12) read $G_{\text{flat}} (\Phi^\top \Phi + \lambda I_{r_e r_{\text{in}}}) = \tilde{R}^\top \Phi$, with unique minimizer

$$G_{\text{flat}}^* = \tilde{R}^\top \Phi (\Phi^\top \Phi + \lambda I_{r_e r_{\text{in}}})^{-1} = \tilde{R}^\top (\Phi \Phi^\top + \lambda I_T)^{-1} \Phi,$$

where the second equality is the Woodbury push-through (1). Either form yields the same $G_{\text{flat}}^* \in \mathbb{R}^{r_{\text{out}} \times r_e r_{\text{in}}}$, and we always solve whichever side has the smaller inversion: $T \times T$ in the typical batched-editing regime ($T \sim 50$ in our experiments, $r_e r_{\text{in}}$ in the thousands), and $(r_e r_{\text{in}}) \times (r_e r_{\text{in}})$ when T is large. The contrast with §3.1 is sharp: the unstructured Woodbury solve carried per-edit design vectors of dimension $E d_{\text{hidden}}$, and the global one-shot solve required factorizing a system of size $E d_{\text{hidden}} \times E d_{\text{hidden}}$. The Tucker reparameterization shrinks both the optimization variable and the per-edit witness by orders of magnitude, while the Woodbury identity preserves the small inversion size in batched mode.

Writeback. Given G_{flat}^* , the per-expert raw-space update is reconstructed via (11) and composed with the per-expert null-space projector to yield the actual weight increment

$$W_j \leftarrow W_j + U_{\text{out}} \left(\sum_{a=1}^{r_e} U_e[j, a] G_a^* \right) U_{\text{in}}^\top P_j. \quad (13)$$

For backbones whose down-projection is stored in transposed packed layout (e.g. Qwen3’s `down_proj` of shape $[E, d_{\text{hidden}}, d_{\text{model}}]$), the increment in (13) is transposed before assignment; for `ModuleList`-style experts, the assignment is direct into `experts[j].down_proj.weight`. Additional ablation on presence of null-space projection in Appendix C.3 shows it’s necessity.

Spreading updates. Iterating (13) across the critical layers $\ell \in \{L_0, \dots, L\}$ with the MEMIT-style residual schedule of (10) leads to calculating $G^{*,L}$ only at the last layer L and spreading it across previous layers from editing set with the same schedule:

$$G^{*,\ell} = \frac{G^{*,L}}{L - \ell + 1}, \quad \hat{\Delta}^{\ell,*} = U_{\text{out}}^\ell \left(\sum_{a=1}^{r_e} U_e^\ell[j, a] G_a^{*,\ell} \right) (U_{\text{in}}^\ell)^\top P_j^\ell, \quad (14)$$

Doing so, factors $U_{\text{in}}^\ell, U_{\text{out}}^\ell, U_e^\ell$ return weight perturbations into each layer’s space and provide correct update, while saving time up to n times, where n is a number of edited layers.

4 Experiments

Model	Method	COUNTERFACT				ZsRE			
		Eff.↑	Gen.↑	Spe.↑	Uti.↑	Eff.↑	Gen.↑	Spe.↑	Uti.↑
Qwen3-30B-A3B	Pre-edited	13.30±0.34	15.10±0.31	84.45±0.24	37.62	41.30±0.29	40.50±0.28	40.91±0.27	40.90
	FT	80.70±0.39	63.95±0.43	41.44±0.39	62.03	6.44±0.14	6.13±0.14	2.15±0.06	4.91
	FT-L	82.40±0.38	22.75±0.33	71.48±0.25	58.88	44.19±0.29	42.46±0.29	41.92±0.27	42.86
	AdaLoRA	51.90±0.50	49.75±0.40	48.10±0.26	49.92	3.66±0.09	3.60±0.09	4.68±0.10	3.98
	UnKE	89.30±0.31	<u>82.85±0.33</u>	48.15±0.33	73.43	31.43±0.28	29.78±0.27	25.30±0.23	28.84
	MoEEdit	97.90±0.14	86.50±0.30	83.45±0.23	89.28	75.29±0.28	67.26±0.32	43.18±0.27	61.91
	MoTE	<u>97.00±0.17</u>	82.60±0.33	<u>79.57±0.26</u>	<u>86.39</u>	<u>72.60±0.28</u>	<u>63.93±0.32</u>	<u>42.67±0.28</u>	<u>59.73</u>
GPT-OSS-20B	Pre-edited	11.80±0.32	14.70±0.31	84.53±0.24	37.01	33.20±0.28	32.14±0.28	28.02±0.00	31.12
	FT	83.40±0.37	58.40±0.42	55.72±0.33	65.84	25.57±0.28	23.41±0.26	17.61±0.21	22.20
	FT-L	73.80±0.44	43.10±0.48	59.75±0.33	58.88	32.75±0.29	33.09±0.30	30.06±0.26	31.97
	AdaLoRA	62.40±0.48	<u>55.00±0.42</u>	43.65±0.34	53.68	43.46±0.30	42.96±0.30	<u>33.60±0.24</u>	40.01
	UnKE	78.00±0.41	44.40±0.42	73.91±0.28	65.44	46.58±0.31	43.99±0.31	31.40±0.26	40.66
	MoEEdit	96.90±0.17	38.80±0.41	<u>80.93±0.26</u>	72.21	68.42±0.33	<u>59.15±0.35</u>	33.23±0.27	<u>53.60</u>
	MoTE	<u>94.60±0.22</u>	37.55±0.41	81.85±0.25	<u>71.33</u>	<u>66.42±0.34</u>	60.03±0.35	37.11±0.28	54.52
Qwen3.6-35B-A3B	Pre-edited	15.10±0.33	16.42±0.30	85.93±0.23	39.15	44.28±0.28	43.61±0.27	42.87±0.26	43.59
	FT	84.75±0.36	66.30±0.41	44.92±0.37	65.32	8.15±0.15	7.42±0.14	3.84±0.08	6.47
	FT-L	85.93±0.35	26.81±0.35	73.62±0.24	62.12	47.88±0.28	45.90±0.28	37.56±0.26	43.78
	AdaLoRA	56.42±0.47	52.91±0.39	50.84±0.25	53.39	7.43±0.12	7.05±0.11	6.88±0.11	7.12
	UnKE	87.84±0.29	<u>74.77±0.31</u>	52.10±0.31	71.57	35.82±0.27	33.74±0.26	28.91±0.22	32.82
	MoEEdit	93.40±0.25	78.55±0.36	77.99±0.26	83.31	61.39±0.32	54.89±0.33	40.93±0.27	52.40
	MoTE	<u>89.20±0.31</u>	68.44±0.39	<u>75.33±0.27</u>	<u>77.66</u>	<u>58.38±0.43</u>	<u>51.79±0.22</u>	<u>39.03±0.32</u>	<u>49.73</u>

Table 1: Results on COUNTERFACT and ZsRE. The best results are in **bold**, the second best are underlined

4.1 Setup

Models. Following the MoEEdit [Gu et al., 2026], we evaluate three modern MoE LLMs: **Qwen3-30B-A3B-2507** [Team, 2025] (contains 128 experts; activates top-8 per token), **GPT-OSS-20B** [OpenAI, 2025] (contains 32 experts; activates top-4 per token), and additionally **Qwen3.6-35B-A3B** [Qwen Team, 2026] (contains 256 experts; activates top-8 per token + 1 shared expert). Hyperparameters of our method for each model can be found in Appendix B.

Datasets. We evaluate performance on two common knowledge editing benchmarks: **COUNTERFACT** (single-hop counterfactual edit dataset) presented with MEMIT [Meng et al., 2022b] and **ZsRE** (zero-shot relation extraction) [Levy et al., 2017].

Baselines. We compare our method mostly with MoEEdit framework [Gu et al., 2026] since it is the only known method specifically targeting editing of MoE models. As additional competitors, we utilize simple fine-tuning (**FT**), fine-tuning with L_∞ -norm constraints (**FT-L**) [Zhu et al., 2020], AdaLoRA [Zhang et al., 2023], and UnKE [Deng et al., 2024].

Metrics. Reported metrics are standard for the field [Meng et al., 2022a,b]. They include (i) **Efficacy** (edit success on edited prompts), (ii) **Generalization** (success on paraphrased prompts), and (iii) **Specificity** (locality measured as a success on an unrelated, neighborhood prompts). To measure overall balance between them, we additionally report **Utility** (mean of three main metrics).

4.2 Main results

Main metrics for each model and method are shown in Table 1. Results show that our method provides second best edit quality in all setups and even outperform MoEEdit in some scenarios (e.g. GPT-OSS-20B model and ZsRE dataset). With GPT-OSS-20B model our method show higher locality on both datasets, which means better preserving of original model performance. Loss of 0.9-4.2 points by our method is highly acceptable due to the extreme speedup, which is shown in Table 2.

4.3 Tucker vs no Tucker

In this section we try to directly adapt MEMIT-like multilayer spreading to BCD and Global solution of (6) as shown in (10). Results in Table 2 show that such naive approach fails to perform on par MoEEdit and MoTE. More detailed discussion can be found in Section 3.1.

Model	Method	COUNTERFACT				Time,s ↓
		Eff.↑	Gen.↑	Spe.↑	Uti.↑	
Qwen3-30B-A3B	MoEEdit	97.90±0.14	86.50±0.30	83.45±0.23	89.28	477.0±17.7
	BCD + <i>speedup</i>	83.53±0.33	69.80±0.40	<u>83.58±0.23</u>	78.97	104.6±25.2
	Global + <i>speedup</i>	94.80±0.22	69.65±0.40	83.70±0.23	82.72	<u>81.6±2.6</u>
	MoTE	<u>97.00±0.17</u>	<u>82.60±0.33</u>	79.57±0.26	<u>86.39</u>	76.8±7.7
GPT-OSS-20B	MoEEdit	96.90±0.17	38.80±0.41	80.93±0.26	72.21	469.2±28.0
	BCD + <i>speedup</i>	89.5±0.19	40.85±0.42	81.73±0.25	70.69	123.9±2.0
	Global + <i>speedup</i>	89.3±0.22	<u>40.55±0.43</u>	<u>81.74±0.28</u>	70.53	<u>100.8±2.2</u>
	MoTE	<u>94.60±0.22</u>	37.55±0.41	81.85±0.25	<u>71.33</u>	88.9±1.3
Qwen3.6-35B-A3B	MoEEdit	93.40±0.25	78.55±0.36	77.79±0.26	83.25	717.4±23.8
	BCD + <i>speedup</i>	82.40±0.38	53.75±0.43	81.40±0.24	72.52	208.0±4.4
	Global + <i>speedup</i>	82.30±0.38	54.35±0.43	<u>81.33±0.24</u>	72.66	<u>121.0±4.5</u>
	MoTE	<u>89.20±0.31</u>	<u>68.40±0.40</u>	75.33±0.27	<u>77.64</u>	112.5±1.3

Table 2: Results on editing 1000 facts from COUNTERFACT dataset with different solvers and multi-layer modes. Time is measured when all v^* vectors are already computed. The best results are in **bold**, the second best are underlined. *Speedup* stands for spreading updates as in (14) instead of spreading residuals as in (10).

5 Limitations and discussion

Knowledge editing methods can be used both for lightweight model updates and for poisoning models forcing them into malicious behavior. It naturally arises ethical concerns about usage of such algorithms, so we call for their responsible use.

Limitations of our method MoTE include (i) high computational cost with large batch sizes ($\gg 1000$), (ii) need of computing HOSVD for making Tucker Decomposition.

6 Conclusion

Beyond the immediate practical benefit of a fast, principled editor for MoE LLMs, our results carry a broader message: closed-form, parameter-modifying knowledge editing is not intrinsically tied to dense architectures. With the right algebraic treatment of the layer’s structure, the same family of techniques can be extended to substantially more complex architectures than the dense FFNs in which they were originally developed. We view this as an

encouraging sign that the principled, optimization-based branch of the KE literature can keep pace with the architectural evolution of modern LLMs.

References

- James A Anderson. A simple neural network generating an interactive memory. *Mathematical biosciences*, 14(3-4): 197–220, 1972.
- Lieven De Lathauwer, Bart De Moor, and Joos Vandewalle. A multilinear singular value decomposition. *SIAM journal on Matrix Analysis and Applications*, 21(4):1253–1278, 2000.
- DeepSeek-AI. Deepseek-v4: Towards highly efficient million-token context intelligence, 2026.
- Jingcheng Deng, Zihao Wei, Liang Pang, Hanxing Ding, Huawei Shen, and Xueqi Cheng. Everything is editable: Extend knowledge editing to unstructured data in large language models. *arXiv preprint arXiv:2405.15349*, 2024.
- Nan Du, Yanping Huang, Andrew M Dai, Simon Tong, Dmitry Lepikhin, Yuanzhong Xu, Maxim Krikun, Yanqi Zhou, Adams Wei Yu, Orhan Firat, et al. Glam: Efficient scaling of language models with mixture-of-experts. In *International conference on machine learning*, pages 5547–5569. PMLR, 2022.
- William Jolly Duncan. Lxxviii. some devices for the solution of large sets of simultaneous linear equations: with an appendix on the reciprocation of partitioned matrices. *The London, Edinburgh, and Dublin Philosophical Magazine and Journal of Science*, 35(249):660–670, 1944.
- Junfeng Fang, Houcheng Jiang, Kun Wang, Yunshan Ma, Shi Jie, Xiang Wang, Xiangnan He, and Tat-Seng Chua. Alphaedit: Null-space constrained knowledge editing for language models. *arXiv preprint arXiv:2410.02355*, 2024.
- Mor Geva, Roei Schuster, Jonathan Berant, and Omer Levy. Transformer feed-forward layers are key-value memories. In *Proceedings of the 2021 Conference on Empirical Methods in Natural Language Processing*, pages 5484–5495, 2021.
- Jia-Chen Gu, Hao-Xiang Xu, Jun-Yu Ma, Pan Lu, Zhen-Hua Ling, Kai-Wei Chang, and Nanyun Peng. Model editing harms general abilities of large language models: Regularization to the rescue. In *Proceedings of the 2024 Conference on Empirical Methods in Natural Language Processing*, pages 16801–16819, 2024.
- Yupu Gu, Rongzhe Wei, Andy Zhu, and Pan Li. Moedit: Efficient and routing-stable knowledge editing for mixture-of-experts llms. *arXiv preprint arXiv:2602.10965*, 2026.
- Yuxuan Gu, Wuyang Zhou, Giorgos Iacovides, and Danilo Mandic. Tensorllm: Tensorising multi-head attention for enhanced reasoning and compression in llms. In *2025 International Joint Conference on Neural Networks (IJCNN)*, pages 1–8. IEEE, 2025.
- Akshat Gupta, Dev Sajnani, and Gopala Anumanchipalli. A unified framework for model editing. In *Findings of the Association for Computational Linguistics: EMNLP 2024*, pages 15403–15418, 2024.
- William W Hager. Updating the inverse of a matrix. *SIAM review*, 31(2):221–239, 1989.
- Tom Hartvigsen, Swami Sankaranarayanan, Hamid Palangi, Yoon Kim, and Marzyeh Ghassemi. Aging with grace: Lifelong model editing with discrete key-value adaptors. *Advances in Neural Information Processing Systems*, 36:47934–47959, 2023.
- Tamara G Kolda and Brett W Bader. Tensor decompositions and applications. *SIAM review*, 51(3):455–500, 2009.

- Dmitry Lepikhin, HyoukJoong Lee, Yuanzhong Xu, Dehao Chen, Orhan Firat, Yanping Huang, Maxim Krikun, Noam Shazeer, and Zhifeng Chen. Gshard: Scaling giant models with conditional computation and automatic sharding. *arXiv preprint arXiv:2006.16668*, 2020.
- Omer Levy, Minjoon Seo, Eunsol Choi, and Luke Zettlemoyer. Zero-shot relation extraction via reading comprehension. In *Proceedings of the 21st Conference on Computational Natural Language Learning (CoNLL 2017)*, pages 333–342, 2017.
- Xiaopeng Li, Shasha Li, Shezheng Song, Jing Yang, Jun Ma, and Jie Yu. Pmet: Precise model editing in a transformer. In *Proceedings of the AAAI Conference on Artificial Intelligence*, volume 38, pages 18564–18572, 2024.
- Yi Li, Zhichun Guo, Miao Yin, and Bingzhe Li. Lestd: Llm compression via learning-based sparse tensor decomposition. In *The Fourteenth International Conference on Learning Representations*, 2026.
- Yun Luo, Zhen Yang, Fandong Meng, Yafu Li, Jie Zhou, and Yue Zhang. An empirical study of catastrophic forgetting in large language models during continual fine-tuning. *IEEE Transactions on Audio, Speech and Language Processing*, 2025.
- Jun-Yu Ma, Jia-Chen Gu, Zhen-Hua Ling, Quan Liu, and Cong Liu. Untying the reversal curse via bidirectional language model editing. *arXiv preprint arXiv:2310.10322*, 2023.
- Kevin Meng, David Bau, Alex Andonian, and Yonatan Belinkov. Locating and editing factual associations in gpt. *Advances in neural information processing systems*, 35:17359–17372, 2022a.
- Kevin Meng, Arnab Sen Sharma, Alex Andonian, Yonatan Belinkov, and David Bau. Mass-editing memory in a transformer. *arXiv preprint arXiv:2210.07229*, 2022b.
- Eric Mitchell, Charles Lin, Antoine Bosselut, Chelsea Finn, and Christopher D Manning. Fast model editing at scale. *arXiv preprint arXiv:2110.11309*, 2021.
- Gleb Molodtsov, Alexander Miasnikov, and Aleksandr Beznosikov. Hierarchical mixture-of-experts with two-stage optimization, 2026. URL <https://arxiv.org/abs/2605.08292>.
- OpenAI. gpt-oss-120b & gpt-oss-20b model card, 2025. URL <https://arxiv.org/abs/2508.10925>.
- Ivan Peshekhonov, Aleksey Arzhantsev, and Maxim Rakhuba. Training a tucker model with shared factors: a riemannian optimization approach. In *International Conference on Artificial Intelligence and Statistics*, pages 3304–3312. PMLR, 2024.
- Qwen Team. Qwen3.6-35B-A3B: Agentic coding power, now open to all, April 2026. URL <https://qwen.ai/blog?id=qwen3.6-35b-a3b>.
- Noam Shazeer, Azalia Mirhoseini, Krzysztof Maziarz, Andy Davis, Quoc Le, Geoffrey Hinton, and Jeff Dean. Outrageously large neural networks: The sparsely-gated mixture-of-experts layer. *arXiv preprint arXiv:1701.06538*, 2017.
- Kai Sun, Yifan Xu, Hanwen Zha, Yue Liu, and Xin Luna Dong. Head-to-tail: How knowledgeable are large language models (llms)? aka will llms replace knowledge graphs? In *Proceedings of the 2024 Conference of the North American Chapter of the Association for Computational Linguistics: Human Language Technologies (Volume 1: Long Papers)*, pages 311–325, 2024.
- Qwen Team. Qwen3 technical report, 2025. URL <https://arxiv.org/abs/2505.09388>.
- Ledyard R Tucker. Implications of factor analysis of three-way matrices for measurement of change. *Problems in measuring change*, 15(122-137):3, 1963.

- Peng Wang, Zexi Li, Ningyu Zhang, Ziwen Xu, Yunzhi Yao, Yong Jiang, Pengjun Xie, Fei Huang, and HuaJun Chen. Wise: Rethinking the knowledge memory for lifelong model editing of large language models. *Advances in Neural Information Processing Systems*, 37:53764–53797, 2024a.
- Song Wang, Yaochen Zhu, Haochen Liu, Zaiyi Zheng, Chen Chen, and Jundong Li. Knowledge editing for large language models: A survey. *ACM Computing Surveys*, 57(3):1–37, 2024b.
- XU Yuebin, Yanhong Wang, Xuemei Peng, Hui Zang, Chen Minghao, Pengfei Xia, and Zeyi Wen. Td-moe: Tensor decomposition for moe models. In *The Fourteenth International Conference on Learning Representations*.
- Qingru Zhang, Minshuo Chen, Alexander Bukharin, Nikos Karampatziakis, Pengcheng He, Yu Cheng, Weizhu Chen, and Tuo Zhao. Adalora: Adaptive budget allocation for parameter-efficient fine-tuning. *arXiv preprint arXiv:2303.10512*, 2023.
- Zhongyu Zhao, Menghang Dong, Rongyu Zhang, Wenzhao Zheng, Yunpeng Zhang, Huanrui Yang, Dalong Du, Kurt Keutzer, and Shanghang Zhang. Factorllm: Factorizing knowledge via mixture of experts for large language models. *arXiv preprint arXiv:2408.11855*, 2024.
- Chen Zhu, Ankit Singh Rawat, Manzil Zaheer, Srinadh Bhojanapalli, Daliang Li, Felix Yu, and Sanjiv Kumar. Modifying memories in transformer models. *arXiv preprint arXiv:2012.00363*, 2020.

Appendix

Supplementary Materials for *Scalable Knowledge Editing for Mixture-of-Experts LLMs via Tensor-Structured Updates*

A Metrics measurement

A.1 ZsRE Evaluation Protocol

Following prior work on model editing, we define a language model \mathcal{M} , an edit request (s_i, r_i) , a desired target response o_{new} , and the model’s original prediction o_{true} .

Efficacy. Edit success measures whether the edited model greedily predicts the target answer on the modified prompt:

$$\mathbb{E}_i \left[\mathbf{1} \left(o_{\text{new}} = \arg \max_t P_{\mathcal{M}}(t \mid (s_i, r_i)) \right) \right].$$

Generalization. We evaluate whether the edit transfers to paraphrased variants $\widehat{\mathcal{P}}(s_i, r_i)$ of the original prompt:

$$\mathbb{E}_i \left[\mathbf{1} \left(o_{\text{new}} = \arg \max_t P_{\mathcal{M}}(t \mid \widehat{\mathcal{P}}(s_i, r_i)) \right) \right].$$

Specificity. Locality preservation quantifies whether unrelated prompts $\mathcal{U}(s_i, r_i)$ remain unaffected after editing:

$$\mathbb{E}_i \left[\mathbf{1} \left(o_{\text{true}} = \arg \max_t P_{\mathcal{M}}(t \mid \mathcal{U}(s_i, r_i)) \right) \right].$$

A.2 CounterFact Evaluation Protocol

For CounterFact, we adopt probability-based metrics under the same setup (s_i, r_i) with target answer o_{new} and original prediction o_{true} .

Efficacy. This metric evaluates whether the edited model assigns higher likelihood to the target answer than to the original prediction:

$$\mathbb{E}_i [P_{\mathcal{M}}(o_{\text{new}} \mid (s_i, r_i)) > P_{\mathcal{M}}(o_{\text{true}} \mid (s_i, r_i))].$$

Generalization. We measure whether paraphrased prompts $\widehat{\mathcal{P}}(s_i, r_i)$ preserve the edited knowledge:

$$\mathbb{E}_i \left[P_{\mathcal{M}}(o_{\text{new}} \mid \widehat{\mathcal{P}}(s_i, r_i)) > P_{\mathcal{M}}(o_{\text{true}} \mid \widehat{\mathcal{P}}(s_i, r_i)) \right].$$

Specificity. For neighboring prompts $\mathcal{U}(s_i, r_i)$ involving related but distinct entities, specificity measures whether the original behavior is preserved:

$$\mathbb{E}_i [P_{\mathcal{M}}(o_{\text{true}} \mid \mathcal{U}(s_i, r_i)) > P_{\mathcal{M}}(o_{\text{new}} \mid \mathcal{U}(s_i, r_i))].$$

B Methods hyperparameters

Hardware and Precision. All experiments are executed on a single machine equipped with an NVIDIA H200 GPU. Model parameters are stored in BF16 precision to reduce memory usage, while all optimizer states, collected activations and gradient updates are maintained in FP32 for improved numerical stability.

Fine-Tuning Baselines. We evaluate both standard fine-tuning (FT) and constrained fine-tuning (FT-L). The FT-L variant restricts the magnitude of parameter updates through a L_∞ -norm constraint ε .

For all three models Qwen3-30B-A3B, GPT-OSS-20B and Qwen3.6-35B-A3B we use $\varepsilon = 10^{-3}$ and a learning rate of 10^{-3} . Parameter updates are applied to last layer presented in Table 3.

Training is conducted for 25 epochs with both weight decay and KL regularization disabled.

UnKE. Since UnKE relies on a two-stage optimization procedure, we configure separate hyperparameters for each phase.

For both Qwen models, the first stage uses a learning rate of 5×10^{-1} with 25 optimization steps and weight decay 10^{-3} . The second stage adopts a learning rate of 2×10^{-4} for 50 additional steps.

For GPT-OSS-20B, the first stage also employs a learning rate of 5×10^{-1} but increases the number of optimization steps to 50, while retaining the same weight decay coefficient. The second stage uses a learning rate of 10^{-4} with 50 optimization steps.

For consistency, all UnKE updates are restricted to the same last layer, as the other baselines. Optimization is performed on the final subject token, following the original structured editing setup.

AdaLoRA. For AdaLoRA, trainable adapters are inserted into all transformer layers. We set the scaling factor $\alpha = 32$ and rank $r = 8$.

The learning rate is set to 5×10^{-3} for Qwen models and 5×10^{-4} for GPT-OSS-20B. Optimization is performed for 25 update steps for all models.

MoEEdit. Layers modified with this method are the same as we show in Table 3.

On Qwen3-30B-A3B, optimization is performed for 25 steps with learning rate 0.1 and 4 Block Coordinate Descent (BCD) iterations. For Qwen3.6-35B-A3B we reduce number of iterations by half due to twice as large number of experts. For GPT-OSS-20B, we use 50 optimization steps, learning rate 0.2, and 10 BCD iterations.

For all models, we set the regularization coefficient $\lambda = 1$ and the KL penalty weight to 0.0625.

To estimate the covariance matrix used in null-space projection, we sample 100K activations. The projection threshold is fixed to 0.02.

MoTE. For this method we utilize the same target vector v^* as for MoEEdit, so all related parameters remain the same. Main differences are shown in Table 3.

Model	λ	Layers	$\varepsilon_{\text{whitening}}$
Qwen3-30B-A3B	0.1	3, 4, 5, 6, 7	1×10^{-5}
GPT-OSS-20B	1	3, 4, 5	1×10^{-2}
Qwen3.6-35B-A3B	0.01	3, 4, 5, 6	1×10^{-5}

Table 3: Hyperparameters for MoTE method

C Additional Experiments

C.1 Routing shift results

Following [Gu et al., 2026], we conduct routing shift distribution analysis on each model and **COUNTERFACT** dataset. We perform 1000 edits with batch size 50 and measure routing similarity (RS) on both editing set and preserved 1000 edits set, averaging score over windows of 10 layers. Results in Table 4 show that our method

outperforms all methods except MoEEEdit. The most probable reason is Tucker Decomposition itself, because it projects inputs and outputs into core space, which shifts the distribution by design.

Model	Method	Editing Set RS \uparrow			Preservation Set RS \uparrow		
		Early	Middle	Late	Early	Middle	Late
Qwen3-30B-A3B	FT	23.57	26.58	29.98	24.72	27.45	30.97
	FT-L	47.01	51.20	53.68	48.80	50.17	53.45
	AdaLoRA	16.63	24.11	27.00	16.38	23.84	26.60
	UnKE	52.46	44.12	44.80	49.90	41.91	43.84
	MoEEEdit	86.62	88.16	89.93	87.02	88.55	90.22
	Ours	<u>59.82</u>	<u>69.11</u>	<u>73.88</u>	<u>67.41</u>	<u>69.83</u>	<u>66.46</u>
GPT-OSS-20B	FT	31.75	28.09	35.25	32.94	28.10	34.98
	FT-L	60.51	57.01	64.95	61.30	57.11	64.12
	AdaLoRA	22.94	18.00	25.91	22.11	19.06	25.28
	UnKE	57.15	53.64	60.86	57.77	53.15	60.26
	MoEEEdit	77.37	75.56	80.83	78.00	76.13	80.53
	Ours	<u>72.06</u>	<u>68.95</u>	<u>75.01</u>	<u>72.38</u>	<u>68.78</u>	<u>74.83</u>
Qwen3.6-35B-A3B	FT	33.83	30.27	37.39	34.45	30.94	36.98
	FT-L	62.92	59.15	66.63	63.48	59.80	66.12
	AdaLoRA	24.08	20.49	27.77	24.61	21.06	27.28
	UnKE	59.34	55.02	62.81	59.89	55.55	62.26
	MoEEEdit	79.00	77.20	82.50	79.50	77.55	82.05
	Ours	<u>73.52</u>	<u>70.45</u>	<u>76.55</u>	<u>74.02</u>	<u>70.48</u>	<u>76.03</u>

Table 4: Routing similarity before and after edit on editing and preservation sets. For Qwen model Early Middle and Late sites are layer 11-20, 21-30 and 31-40, for GPT-OSS: 5-9, 10-14 and 15-19, respectively. Best results are in **bold**, second best are underlined

C.2 Whitening ablation

Following results of [Yuebin et al.], we made an ablation on whitening type for each model. As for other experiments, we make 1000 edits from **COUNTERFACT** dataset with batch size 50 and other hyperparameters exactly matching those from Appendix B. Results in Table 5 show that using only *in* whitening show best performance and it’s absence lead to huge model degradation. *Out* whitening in original implementation with random gradients doesn’t yield any improvement and even brings slight decline in main metrics in combination with *in* whitening.

C.3 Null-space ablation

In this section we compare performance of MoTE method with enabled and disabled null-space projection. From results shown in Table 6 and evaluation protocol of **COUNTERFACT A**, we can conclude, that without null-space projection our method turn model into a random predictor which chooses between o_{true} and o_{new} . It shows the urgency of this component for preserving model overall performance.

Model	Whitening type	COUNTERFACT			
		Eff.↑	Gen.↑	Spe.↑	Uti.↑
Qwen3-30B-A3B	None	63.50±0.48	61.15±0.42	66.45±0.31	63.70
	Out	66.50±0.47	61.95±0.42	86.06 ±0.31	71.50
	In	97.00 ±0.17	82.60 ±0.33	<u>79.57</u> ±0.26	86.39
	Both	<u>96.80</u> ±0.18	<u>82.55</u> ±0.32	79.47±0.26	<u>86.27</u>
GPT-OSS-20B	None	41.70±0.49	37.10±0.42	65.50±0.33	48.10
	Out	45.87±0.50	36.80±0.41	66.32±0.33	49.66
	In	94.60 ±0.22	<u>37.55</u> ±0.41	81.85 ±0.25	<u>71.33</u>
	Both	<u>94.50</u> ±0.23	38.30 ±0.42	<u>81.76</u> ±0.25	71.52
Qwen3.6-35B-A3B	None	<u>82.50</u> ±0.38	<u>73.00</u> ±0.37	64.50±0.32	73.33
	Out	82.10±0.38	73.95 ±0.37	65.07±0.30	73.71
	In	89.20 ±0.31	68.44±0.39	<u>75.33</u> ±0.27	77.66
	Both	88.50±0.32	68.00±0.40	75.52 ±0.27	<u>77.34</u>

Table 5: Results of editing 1000 facts from **COUNTERFACT** dataset with different whitening types. Best results are in **bold**, second best are underlined

Model	Null-space	COUNTERFACT			
		Eff.↑	Gen.↑	Spe.↑	Uti.↑
Qwen3-30B-A3B	✓	97.00±0.17	82.60±0.33	79.57±0.26	86.39
	×	49.60±0.50	49.0±0.36	48.91±0.21	49.17
GPT-OSS-20B	✓	94.60±0.22	37.55±0.41	81.85±0.25	71.33
	×	50.10±0.50	50.90±0.47	48.44±0.45	49.81
Qwen3.6-35B-A3B	✓	89.20±0.31	68.44±0.39	<u>75.33</u> ±0.27	77.66
	×	49.90±0.52	51.1±0.48	50.3±0.55	50.43

Table 6: Results of editing 1000 facts from **COUNTERFACT** dataset with MoTE method with *in* whitening and with or without null-space projection